Development of a space-flight ADR providing continuous cooling at 50 mK with heat rejection at 10 K

James Tuttle[1], Edgar Canavan[1], Hudson DeLee[1], Michael DiPirro[1], Amir Jahromi[1], Bryan James[1], Mark Kimball[1], Peter Shirron[1], Dan Sullivan[1], and Eric Switzer[2]

[1]*NASA Goddard Space Flight Center, Code 552, Greenbelt, MD 20771 USA*
[2]*NASA Goddard Space Flight Center, Code 665, Greenbelt, MD 20771 USA*

E-mail: james.g.tuttle@nasa.gov

Abstract. Future astronomical instruments will require sub-Kelvin detector temperatures to obtain high sensitivity. In many cases large arrays of detectors will be used, and the associated cooling systems will need performance surpassing the limits of present technologies. NASA is developing a compact cooling system that will lift heat continuously at temperatures below 50 mK and reject it at over 10 K. Based on adiabatic demagnetization refrigerators (ADRs), it will have high thermodynamic efficiency and vibration-free operation with no moving parts. It will provide more than 10 times the current flight ADR cooling power at 50 mK and will also continuously cool a 4 K stage for instruments and optics. In addition, it will include an advanced magnetic shield resulting in external field variations below 5 μT. We describe the cooling system here and report on the progress in its development.

1. Introduction

Several past, and many future, astronomical instruments require cooling to sub-Kelvin temperatures to obtain high sensitivity. Newer generations of detector arrays need several μW of cooling at temperatures of 50 mK or lower. Sub-Kelvin temperatures in space are produced by a combination of mechanical cryocoolers at the upper temperature end and specialized sub-Kelvin coolers at the cold end. An adiabatic demagnetization refrigerator (ADR), having a thermodynamic efficiency close to Carnot, is the most efficient way to produce sub-Kelvin temperatures. It provides cyclic cooling by first raising the magnetic field in a paramagnetic material, removing the resulting heat from the material through a closed thermal switch, then isolating it by opening the switch, and cooling it by reducing the field. Our team, at NASA's Goddard Space Flight Center (GSFC), invented a method to produce high-heat-lift continuous cooling with a multi-stage continuous ADR (CADR)[1]. We demonstrated a laboratory CADR with 6.5 μW of continuous cooling at 50 mK, a significant improvement over the single-shot 0.7 μW cooling provided for about 40 hours per cycle on ASTRO-H/SXS[2]. Our CADR[3] alternatively provides 31 μW at 100 mK, compared to the 0.2 μW of cooling achieved on Planck. It rejects heat to a cryocooler at temperatures as high as 4.5 K.

In addition to detector cooling, several proposed far infrared space observatories require telescopes

Table 1. The expected cooling requirements for future missions, the target performance of our proposed CADR, and the current state-of-the-art (ASTRO-H).

Performance metrics	Requirements	Current SOA	Proposed CADR
Cold Stage Operating temp. (mK)	≤ 50	50	< 50
Cold Stage temp. stability (μK)	1	1	< 1
Cold Stage Cooling power (μW)	2	0.5	> 6
Warmer Stage Stability at Operating Temp. (mK@K)	1@4-6	1@4.5	1@4
Telescope Cooling (power@temp., mW@K)	100@4-6	20@4.5	>20@4 K
Mag. Field at detector assembly (μT)	5	7500	< 5
Allowable vibration levels (milli Newtons, mN)	0.001	5	~ 0
Lifetime (years)	> 5	> 5	> 5

to be at 2 - 6 K to limit self-emission. This is much colder than the approximately 30 K that can be achieved via passive cooling, as in the James Webb Space Telescope (JWST).

Many space observatories require extremely stable pointing. The CADR, which has no moving parts, is vibration free, but it is just part of a cooling chain. Currently, the CADR rejects its heat at 4 Kelvin, limiting the choice of upper stage coolers to linear piston cryocoolers. Jitter caused by such coolers has been a problem for recent astrophysics missions. Miniature turbo-Brayton coolers offer a solution to this problem, as was demonstrated by the 70 Kelvin cooler for the Hubble/NICMOS instrument[4]. The extremely high-frequency vibrations produced by the turbine are almost completely damped out by typical spacecraft structures. There are difficulties extending this technology to 4 Kelvin, but an engineering unit has recently demonstrated significant cooling power at 10 Kelvin. Thus, extending the CADR heat rejection temperature from 4 to 10 Kelvin will enable sub-Kelvin detectors in observatories with tight pointing requirements.

With NASA funding between 2002 and 2010, Superconducting Systems, Inc. (SSI) developed a relatively lightweight, low-current superconducting magnet capable of producing a 4 Tesla central field at 10 K[5]. This magnet enables the production of an ADR which cools at 4 K and rejects heat at 10 K. We demonstrated this concept with the prototype SSI magnet and spare ADR parts from our lab. Now it is possible to raise our CADR's heat rejection temperature to 10K, and coupling it with a turbo-Brayton cooler could produce 300 K to 50 mK zero-vibration continuous cooling.

In 2016, our group at GSFC submitted a proposal to NASA Headquarters to extend our laboratory CADR's heat rejection to 10 K, add a 4 K continuous cooling stage, and advance the technology's maturity so that it would be space-flight-ready by the end of 2019. We were selected for funding under NASA's Cosmic Origins program, and our development effort began in January, 2017. Table 1 shows the target performance of our proposed CADR along with the expected cooling requirements for future missions and the current state-of-the-art (ASTRO-H). It should be noted that the ASTRO-H ADR did not provide continuous cooling, but had a hold time of about 40 hours between recycling events[6]. Our target cooling power and temperature stability at 50 mK will match those of our lab CADR, with stiffer and stronger parts, as needed, to survive launch vibrations. For practical reasons, we will demonstrate less than the required continuous cooling power at 4 K, but this could be increased later by adding additional stages. We will also advance the magnetic shielding beyond that of previous ADR's, with an overall shield around our system to keep stray fields below 5 μT. This is important, since time-varying fields from ADR magnets could have detrimental effects on the sensitivity of nearby detectors.

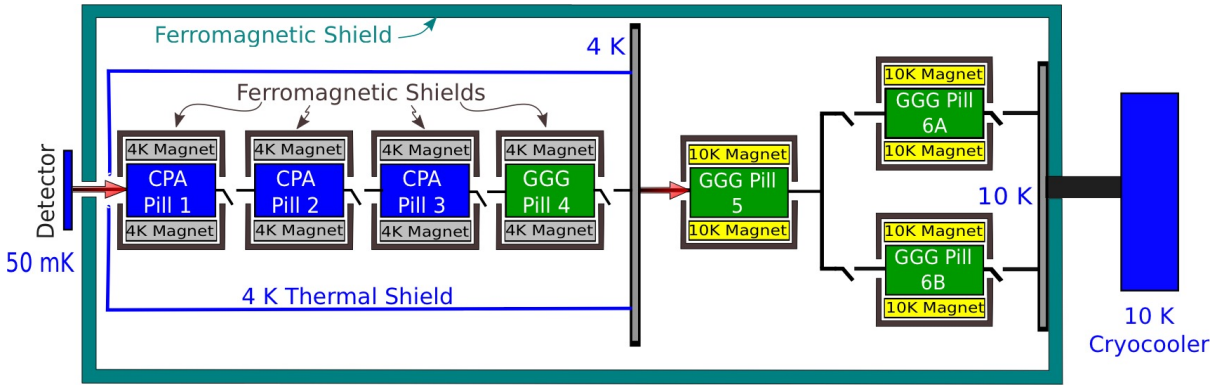

Figure 1. A schematic representation of our proposed CADR.

2. The Proposed CADR

Figure 1 shows our proposed CADR schematically. It consists of seven ADR stages, each being a paramagnetic "pill" suspended by tensioned Kevlar ropes inside a superconducting magnet. These stages are grouped into two different CADR's, which will be tested separately before integration into the overall system. The left side of the image is the 4-stage 0.05 to 4 K CADR, an improved version of our lab CADR[3]. Its magnets are wound with niobium-titanium wire and are thermally and structurally attached to the continuous 4 K stage. The first three pills are chrome potassium alum (CPA), and the fourth is gadolinium gallium garnet (GGG). The stages are thermally connected in series via heat switches and copper straps. The switch between the first two stages is a superconducting rod surrounded by a Helmholtz coil. It has a very low thermal conductance until the coil is energized, driving the rod normal. In the normal state the rod's conductance increases by a factor of 10^5, closing the thermal switch[7]. All other heat switches in the CADR are passive gas gap switches, which will be discussed later. The first stage, on the very left, remains continuously at 0.05 Kelvin. The other stage temperatures rise and fall as the heat switches open and close and magnetic fields are raised and lowered. This sequence of events pumps heat from the cold source to the continuous 4 Kelvin stage. Should an additional steady state temperature point be needed, for example for detector harness heat sinking, it is straightforward to add an additional continuous stage. The 4 to 0.05 K CADR is surrounded by a 4 K thermal shield to eliminate the heat load from 10 K thermal radiation.

The 10 to 4 K CADR is on the right side of the image. It includes two parallel stages, 6A and 6B, one of which absorbs heat at 4 Kelvin, while the other dumps heat at just above 10 K to the cryocooler. We plan to have an additional stage, labeled stage 5 in the figure, which remains continuously at 4 K. This stage simplifes the temperature control and enhances the overall cooling at that temperature. The pills in the 4 to 10 K part of the CADR are all GGG. The magnets in the baselined design, installed on the 10 K stage, are duplicates of the prototype SSI 10 K magnet. However, stage 5 could use a 4 K niobium-titanium magnet.

Each magnet in the overall CADR has its own ferromagnetic shield, machined from silicon-iron, to minimize its stray magnetic field and to enhance the field inside the magnet bore. The entire system is surrounded by a second shield which further reduces any field fluctuations caused by the magnets. We expect this to be a 10 K shield, as indicated in the figure, made from a ferromagnetic material such as Cryoperm. Figure 2 shows a preliminary layout concept for the CADR components inside a 35 cm diameter shield. However, it is possible that the required shielding will necessitate a superconducting shield at 4 K, requiring a re-packaging of the CADR components.

The 4 to 0.05 K part of our CADR is very similar to our laboratory CADR [1], with a few enhancements to make it space-flight ready. Most of its parts are build-to-print copies of our lab CADR's parts, and we will fabricate them over the next two years. However, the 10 to 4 K CADR is a

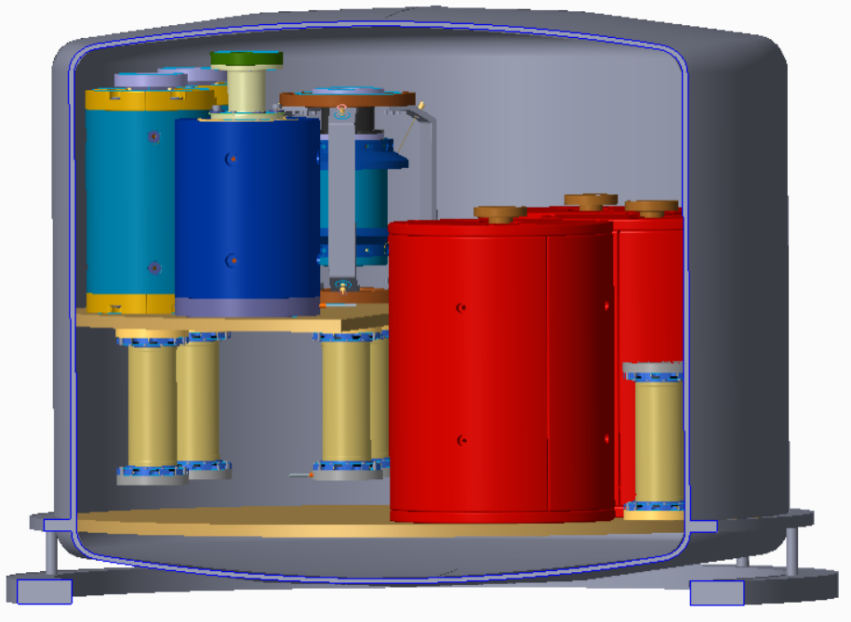

Figure 2. A preliminary model of the full CADR layout inside a 35 cm diameter 10 K magnetic shield. The 4 to 0.05 K CADR is on the left side, and the 10 to 4 K CADR is on the right. For clarity, the 4 K thermal shield and several copper straps and isolating supports are not shown.

much less mature technology, so our highest early priority has been to design and analyze its parts and to test the components already in hand.

3. The 10 K Magnet

A key component in each 10 to 4 K stage is the SSI magnet, shown in Figure 3A. It includes 4 nested coils wound with thin Nb_3Sn wire, assembled inside an aluminum shell. Without a magnetic shield it weighs 1.8 kg, and it produces a 4 Tesla central field with an operating current of 6.5 amps. We performed a detailed structural analysis on the magnet based on design details provided by SSI. Its lowest resonant frequency is above 600 Hz, and no unacceptable stress concentrations were seen during simulated vibrations. Aside from some new attachment holes being added to the outer shell, the 10 K magnets in our CADR should be nearly identical to the prototype.

The prototype magnet had undergone basic performance testing in 2010, and we had used it since then in our lab. For more thorough testing, we installed it on an aluminum stage supported above a cryostat's 3 K cold plate and linked to the cold plate with a copper strap. A heater and thermometer on the stage allowed it to be controlled at the 10 K operating temperature. We installed Nb_3Sn test leads, provided by SSI, between the magnet's internal current leads and our cryostat's cold plate wiring. Voltage taps, attached to the current lead solder joints on the magnet, allowed us to monitor the magnet voltage at all times. Our available power supply could only produce currents up to 5 amps, but we are procuring new ones which can reach the magnet's full 6.5 amp operating current.

Our preliminary testing confirmed that the magnet could be ramped to 5 amps and back to zero amps at rates as fast as 0.1 amp/sec. We also held the magnet at several different steady current values to measure its DC internal resistance. Because the magnet voltage was noisy, significant time-averaging was needed to get precise measurements. We simultaneously monitored the stage control heater power, which dropped as the current increased. The difference between this power and the zero-current power was the ohmic heating in the magnet, from which we could also determine the resistance. The resistance calculated from this thermal measurement matched that determined from the voltage to within the measurement uncertainties. It increased approximately linearly with current from 50 μΩ at 1 amp to 90 μΩ at 5 amps. This resistance is assumed to be due to internal solder

A. 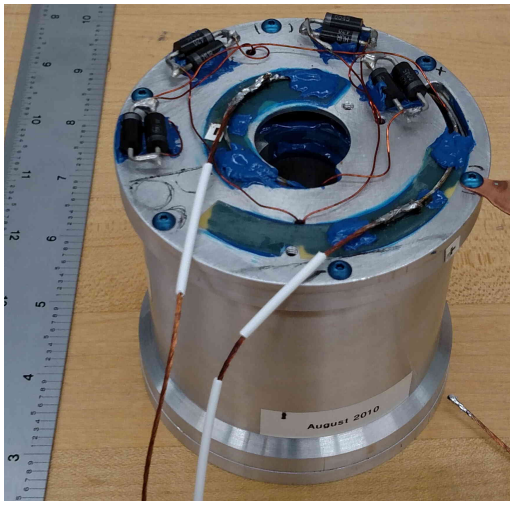

B. 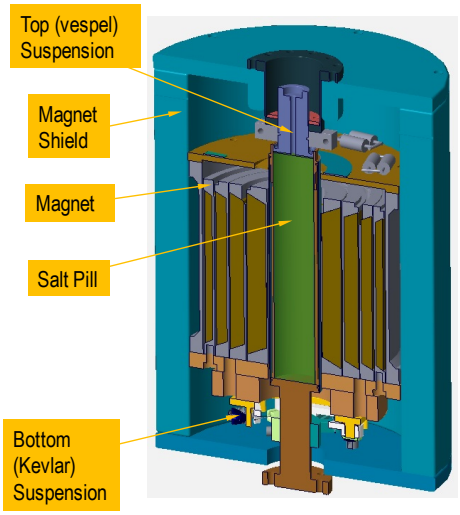

Figure 3. A. The prototype 10 K magnet, developed by SSI. **B.** A single 10 to 4 K ADR stage, showing the salt pill assembly suspended inside the magnet inside its ferromagnetic shield.

joints, and SSI will attempt to reduce it in future versions of the magnet.

We determined the prototype magnet's AC heating during ramp cycles from zero to full field and back to zero field. This was done by computing the stage's controlling power approximately twice every second as the magnet current was cycled. At any time, the sum of the zero-current control power plus the DC ohmic power minus the instantaneous temperature control power was the instantaneous power produced in the magnet. This magnet power, in Watts, was multiplied by the time difference to get the energy generated during a time step. We added up all of these energy values to get the total AC magnet energy per 5 amp cycle. It is only weakly dependent on the ramp rate, indicating that it is dominated by hysteretic heating. To estimate the heating for a full 6.5 amp cycle, we assumed that the power was constant and scaled the energy by the cycle time. This is likely a conservative estimate, however, since hysteretic heating tends to decrease with rising magnet fields. During CADR operation we expect a single magnet's cycle to take about 160 seconds, and it generates about 0.93 Joules per cycle at this rate. With two magnets, each cycling once per 10 minute cycle of the 10 to 4 K CADR, the average magnet heat load at 10 K would be 3 mW. The optional stage 5 magnet would increase this to about 4 mW, which is insignificant compared to the expected cryocooler capacity of several hundred mW at that temperature. As soon as the 10 K magnet's ferromagnetic shield is fabricated, we will perform a similar test on the shielded magnet to determine the additional AC heating in the shield.

4. The 10 to 4 K ADR Stage

Figure 3B shows a cross section of a 10 to 4 K stage, consisting of the salt pill assembly suspended inside the magnet inside its ferromagnetic shield. The shield concentrates the magnetic field external to the magnet itself, minimizing fringe fields at more distant locations. Its cylindrical shell and each of its end caps are made of two separate half-parts, to minimize eddy-current heating. The shield thickness was chosen, via analysis, so that at maximum magnet current its internal field will be below the silicon-iron's 2.1 T saturation level. The magnet is supported inside the shield by radial screws. Experience with lower temperature magnets supported in this way indicates that this will be acceptable structurally and thermally. A salt pill suspension assembly, including tensioned Kevlar ropes, is mounted on the bottom end of the magnet. The other end of the salt pill is held by a thin-walled Vespel part, which attaches to the top of the shield.

The salt pill itself is a single-crystal GGG rod. Magneto-thermal analysis showed that its optimum length is longer than the magnet coil length, as the field extending some distance out of the magnet is

strong enough to produce practical cooling in GGG. The pill is housed inside a slit copper can. This can is part of a copper thermal bus, which extends out of the bottom of the magnet. The can is surrounded by a hermetic stainless steel shell, which is electron-beam welded in place. The pill assembly is closed out at the top by welding on a cylindrical piece with a small central hole running out from the pill volume. After the welding, the gap surrounding the pill is pumped out and filled with helium gas, and the fill hole is sealed hermetically. The gas enhances the pill's thermal contact with the copper bus. The copper thermal bus is held by the Kevlar suspension assembly below the magnet, and the cylindrical pump-out piece at the top attaches to the Vespel structure. All conductive straps running from the pill assembly to heat switches or heat sinks are attached to the pill's copper thermal bus at the bottom.

5. Gas-Gap Heat Switches

Except for the superconducting switches described earlier, all heat switches in all of our ADR's are gas-gap switches. Each consists of two copper thermal buses in close proximity to each other, held in place by a structure which keeps them from touching and isolates them thermally from each other. The volume between them is sealed hermetically from the outside environment and filled initially with gas. The buses have interleaving fins so that heat conducted between them through the gas crosses a short distance over a large area. The gas thermally "shorts" the buses together, closing the heat switch. When conditions are right, a charcoal or sintered-metal getter inside the hermetic gas volume cools to a lower temperature, causing it to adsorb nearly all of the gas and evacuate the volume. This drastically reduces the thermal conduction between the buses, opening the heat switch.

The heat switches which flew on ASTRO-H were "active" switches. They each had a getter located in a separate can plumbed to the main switch volume via a thin-walled tube, which isolated the getter thermally from the main volume. These switches were normally-open, and they were closed by powering a resistive heater on the getter assembly. The resulting getter temperature rise released the gas into the volume between the buses, closing the switch. In contrast, all of the gas-gap switches in our proposed CADR are "passive." Each of their getters is thermally linked to a thermal bus, and it adsorbs or desorbs gas depending on that bus temperature. No heater is required, and proper getter and gas configuration causes these switches to open and close automatically at the correct time in the CADR cycle. Passive switches have been demonstrated successfully in our 4 K to 0.05 K laboratory CADR, but until recently we had never optimized one for operation above 4 K.

Figure 4A shows a cross section view of a passive switch which will be used between stage 6A or 6B and the 10 K stage in our CADR. It contains a charcoal getter, which is the rectangle in the lower left of the image. The switch's slightly-tapered interleaved fins are held apart by a stainless steel shell, which can be seen in the photograph in Figure 4B. The switches between pills 6A and 6B and pill 5 will be very similar to this one, but they will have external getters like those on ASTRO-H. However, these new getters will not be operated by heaters. Instead, they will each be strapped to the salt pill on the opposite side of the 10 to 4 K CADR. Thus, when pill 6A cools to 4 K, the switch connected to pill 6B will open, and vice-versa.

In order for the switch shown in Figure 4 to open and close at the correct getter temperature, it must be filled with the correct pressure of the correct gas. These characteristics depend on the switch volume, the effective surface area of the getter, and the operating temperature. Predicting the optimum fill pressure is difficult, and it ends up being fine-tuned by trial and error. This process is described in detail elsewhere[8]. For the switch shown in Figure 4, we ended up using 250 Torr of ^{3}He gas to tune its on/off temperature to just below 10 K. The resulting switch conductance is shown in Figure 5.

The getter end of the switch will be linked to the stage 6A or 6B salt pill via a thermal strap, and the other end will be linked to the CADR's 10 K stage. When the stage 6 magnetic field is ramped up for recycling, the pill and the switch's getter will warm above 10 K, and the switch will provide 10's of mW/K of conductance. After the stage 6 magnet reaches its full field and the ramping stops, the pill will cool back to 10 K. When the magnet's current is ramped down, cooling the pill to 4 K, the

A. 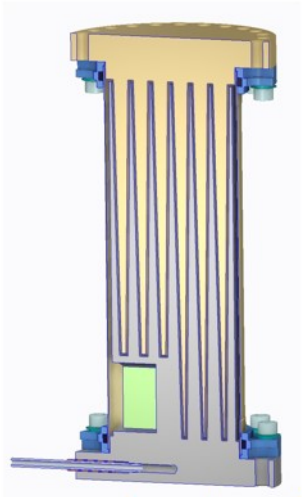 B. 

Figure 4. A. A design model cross section image of a passive gas-gap heat switch switch used between stages 6A or 6B and the 10 K stage, showing the interleaved, slightly tapered copper fins. This particular switch has an internal charcoal getter, which is the rectangle located at the lower left side. **B.** A photograph of this same switch, showing its stainless steel shell.

switch conductance will drop by nearly three orders of magnitude. While the pill is providing cooling at 4 K, less than 0.5 mW of heat will leak from 10 K to the 4 K stage through the switch's shell.

6. Control Algorithm Improvement

An additional goal of our effort is to improve the CADR control algorithm for the continuous 50 mK stage. Since this stage will cool detector arrays, its temperature must be extremely stable. For most of its operation, this is not a problem, and, even using a simple PID control algorithm, temperature stability is typically limited by thermometer noise. However, in the brief (< 10 s) period when the heat switch changes state and the continuous stage switches from magnetizing to demagnetizing, heat flow in the pill must reverse, which is problematic for simple controllers. Using a basic feed-forward algorithm, we have been able to reduce the resulting disturbance to < 100 μK. While reducing such a disturbance at the CADR interface to an acceptable level at the detectors is feasible by a number of methods, it is the best to eliminate it directly at the interface.

To shrink this disturbance into the noise, we will use better control of the heat switch and a better control algorithm. Up to now, superconducting heat switches have been used as binary devices. However, given the geometry of our switch, it should be possible to operate it in the intermediate state, where its conductance can be smoothly modulated. We will combine this capability with a more sophisticated control algorithm based on a thermal model of the system. The parameters of the current feed-forward control algorithm are calculated from a simple lumped parameter model of the CADR. A model that includes thermal diffusion and other detailed effects will be better able to anticipate, and thus cancel, temperature excursions at the control thermometer.

7. Plan Forward

Our plan is to demonstrate a single-stage 10 to 4 K ADR in 2017, a two or three stage 10 to 4 K CADR in 2018, and the full 10 to 0.05 K CADR in 2019. We will develop and test the overall magnetic shield before 2019, if possible. Control algorithm improvement will begin in 2018, and it will be demonstrated during testing in 2019. The complete system will be tested before and after a vibration test in order to demonstrate that is it flight-ready.

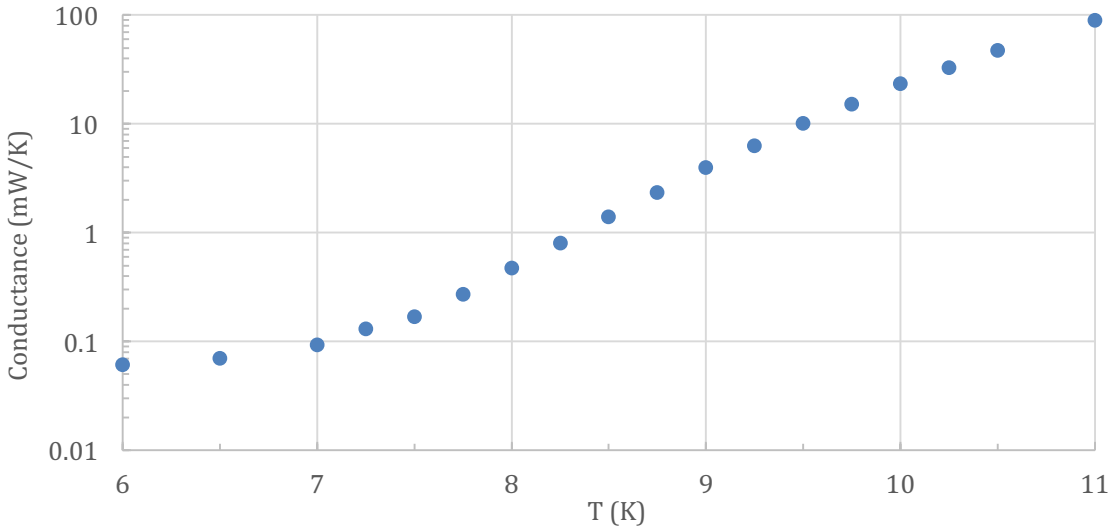

Figure 5. The thermal conductance of the passive gas gap heat swich which will be used between pill 6A or 6B and the 10 K stage.

References

[1] Shirron P *et al*. 2000 *Adv*. *Cryo*. *Eng*. **45** pp 1629-1638.
[2] Shirron P *et al*. 2016 *Proc*. *SPIE* **9905** 99053O.
[3] Shirron P *et al*. 2005 *Proc*. *SPIE* **5904** 5904W.
[4] Nellis G *et al*. 1999 *Proc*. *Int*. *Cryocooler Conference* **10** pp 431-438.
[5] Tuttle J *et al*. 2008 *Cryogenics*, **48** pp 248-252.
[6] Shirron P *et al*. 2016 *Cryogenics*, **74** pp 2-9.
[7] Mueller R *et al*. 1978 *Rev*. *Sci*. *Inst*., **49** pp 515-518.
[8] Kimball M *et al*. 2017 to be published in *Cryogenics*.

Acknowledgements

This work was supported by NASA's Cosmic Origins program.